A low-dimensional framework for interpreting Northern Hemisphere winter extratropical precipitation trends

Ha-Rim Kim[1], Changhyun Yoo[2*], Hyodae Seo[3], and Baek-Min Kim[4]

[1]Institute of Sustainable Earth and Environmental Dynamics, Pukyong National University, Busan, 48513, Republic of Korea
[2]Department of Climate and Energy Systems Engineering, Ewha Womans University, Seoul, 03760, Republic of Korea
[3]Department of Oceanography, University of Hawai'i at Manoa, Honolulu, HI 96822, USA
[4]Division of Earth Environmental System Science, Pukyong National University, Busan, 48513, Republic of Korea

Correspondence to: Changhyun Yoo (cyoo@ewha.ac.kr)

Contents of this file

15

Supplementary Table 1. Summary of CMIP6 models used for historical and SSP5–8.5 simulations in this study.

CMIP6									
Historical Simulation					SSP5-8.5 Simulation				
No.	**Model Name**	**Country**	**Horizontal Resolution**	**Reference**	**No.**	**Model Name**	**Country**	**Horizontal Resolution**	**Reference**
1	CanESM5	Canada	2.81° × 2.81°	Swart et al. (2019)	**1**	CanESM5	Canada	2.81° × 2.81°	Swart et al. (2019)
2	FGOALS-g3	China	2° × 2.25°	Li et al. (2019)	**2**	ACCESS-CM2	Australia	1.88° × 1.25°	Dix et al. (2019)
3	INM-CM4-8	Russia	2° × 1.5°	Volodin et al. (2019)	**3**	ACCESS-ESM1-5		1.88° × 1.25°	Ziehn et al. (2019)
4	GFDL-CM4	USA	1.25° × 1°	Guo et al. (2018)	**4**	AWI-CM-1-1-MR	Germany	0.94° × 0.94°	Semmler et al. (2019)
5	CESM2		1.25° × 0.94°	Danabasoglu and Gokhan (2019)	**5**	BCC-CSM2-MR	China	1.13° × 1.13°	Xin et al. (2019)
6	CESM2-FV2		2.5° × 1.9°		**6**	CESM2-WACCM	USA	1.25° × 0.94°	Danabasoglu and Gokhan (2019)
7	CESM2-WACCM		1.25° × 0.94°		**7**	EC-Earth3	Europe	0.7° × 0.7°	EC-Earth (2019)
8	ACCESS-CM2	Australia	1.88° × 1.25°	Martin et al. (2019)	**8**	EC-Earth3-Veg		0.7° × 0.7°	
9	AWI-ESM-1-1-LR	Germany	1.88° × 1.88°	Danek et al. (2020)	**9**	EC-Earth3-CC		0.7° × 0.7°	
10	MPI-ESM-1-2-HAM		1.88° × 1.88°	Neubauer et al. (2019)	**10**	EC-Earth3-Veg-LR		1.13° × 1.13°	EC-Earth (2020)
11	MPI-ESM1-2-HR		0.94° × 0.94°	Jungclaus et al. (2019)	**11**	INM-CM4-8	Russia	2° × 1.5°	Volodin et al. (2019)
12	MPI-ESM1-2-LR		1.88° × 1.88°	Wieners et al. (2019)	**12**	INM-CM5-0		2° × 1.5°	
13	EC-Earth3	Europe	0.7° × 0.7°	EC-Earth (2019)	**13**	IPSL-CM6A-LR	France	2.5° × 1.26°	Boucher et al. (2019)
14	IITM-ESM	India	1.88° × 1.9°	Choudhury et al. (2019)	**14**	MIROC6	Japan	1.4° × 1.4°	Shiogama et al. (2019)
15	IPSL-CM6A-LR	France	2.5° × 1.26°	Boucher et al. (2019)	**15**	MRI-ESM2-0		1.13° × 1.13°	Yukimoto et al. (2019)
16	MIROC6	Japan	1.4° × 1.4°	Tatebe and Watanabe (2018)	**16**	NorESM2-LM	Norway	2.5° × 1.9°	Seland et al. (2019)
17	MRI-ESM2-0		1.13° × 1.13°	Yukimoto et al. (2019)	**17**	NorESM2-MM		1.25° × 0.94	Bentsen et al. (2019)
18	NorESM2-LM	Norway	2.5° × 1.9°	Seland et al. (2020)	**18**	TaiESM1	Chinese Taibei	1.25° × 0.2°	Lee et al. (2020)
19	NorESM2-MM		1.25° × 0.94°	Bentsen et al. (2019)	**19**	KACE-1-0-G	Republic of Korea	1.88° × 1.25°	Byun et al. (2019)
20	TaiESM1	Chinese Taibei	1.25° × 0.2°	Wang et al. (2021)					
21	KACE-1-0-G	Republic of Korea	1.88° × 1.25°	Byun et al. (2019)					

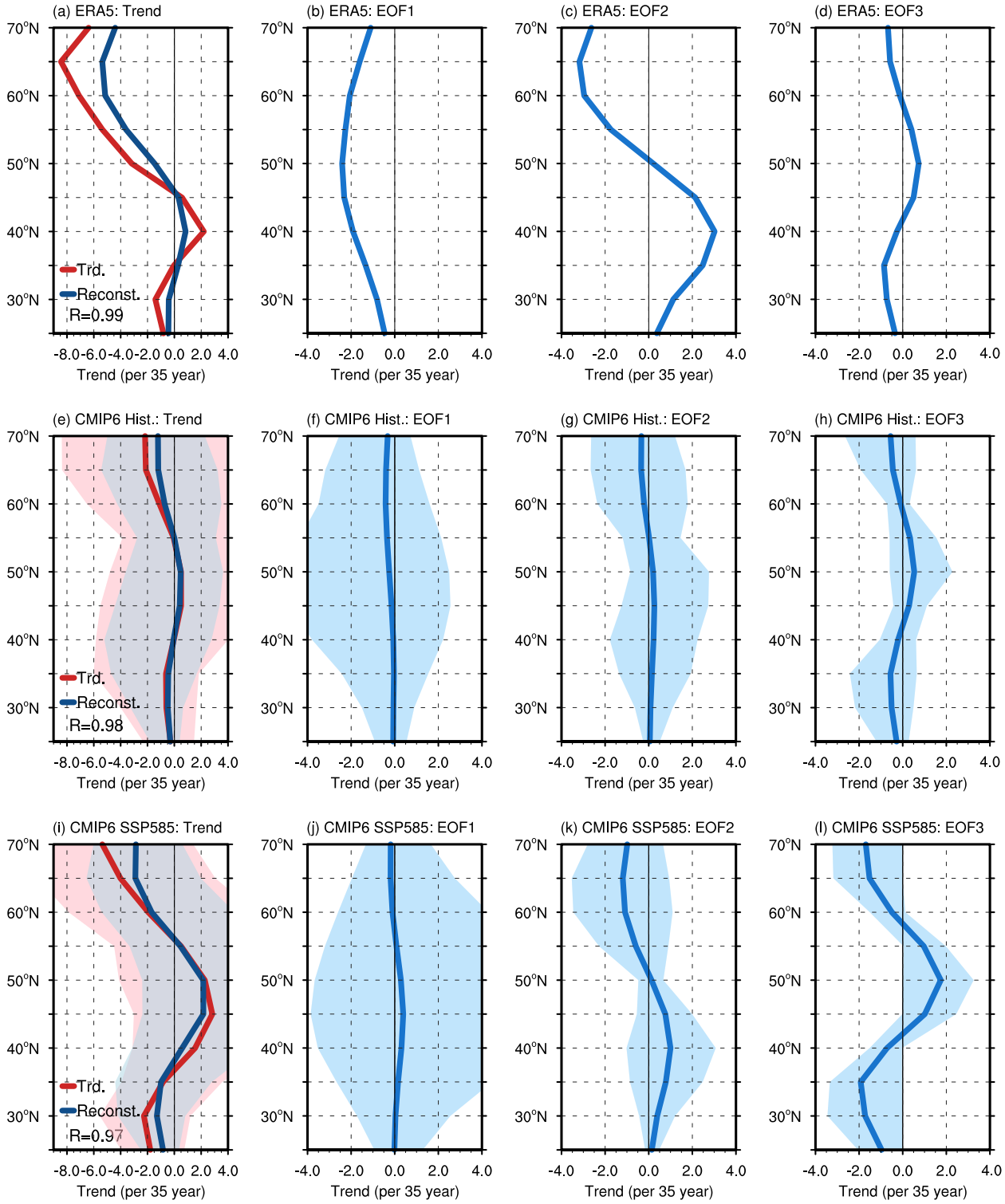

Supplementary Figure 1. Zonal-mean profiles of 500-hPa geopotential height trends and their dynamical reconstructions. Zonal-mean profiles are shown for (a–d) ERA5 (1979–2014), (e–h) the CMIP6 historical multi-model mean (MMM; 21 models, 1979–2014), and (i–l) the CMIP6 SSP585 MMM (19 models, 2015–2100). The first column (a, e, i) compares the original 500-hPa geopotential height (Z500) trends (red) with the dynamical reconstructions (blue) obtained by summing all decomposed Z500 activity components (transient, stationary, and interaction), with pattern correlation coefficients (R) shown in each panel.

The remaining columns show the Z500 trend contributions associated with (b, f, j) EOF1, (c, g, k) EOF2, and (d, h, l) EOF3. Shading in the CMIP6 rows indicates the intermodel spread (minimum to maximum) across individual models.

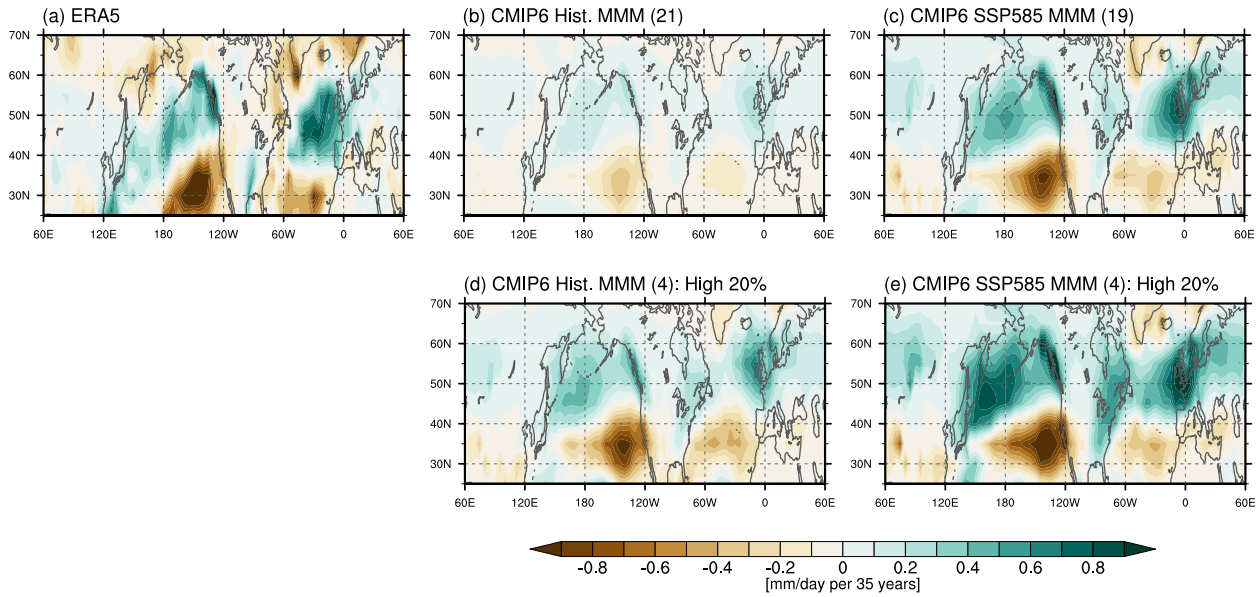

27

28 **Supplementary Figure 2. Induced total precipitation trend reconstructed from all decomposed dynamical components.**
29 Spatial distributions show the induced total precipitation trend obtained by summing the precipitation-trend contributions from all
30 decomposed 500-hPa geopotential-height (Z500) activity components (transient, stationary, and interaction). Results are shown
31 for (a) ERA5 (1979–2014), (b) the CMIP6 historical multi-model mean (MMM; 21 models, 1979–2014), and (c) the CMIP6
32 SSP585 MMM (19 models, 2015–2100). Panels (d) and (e) show the same quantity for the high-PROJ subsets, consisting of four
33 models selected from the top ~20% ranked by PROJ score in the historical and SSP585 ensembles, respectively. Shading
34 indicates the trend magnitude (mm day^{-1} per 35 years).

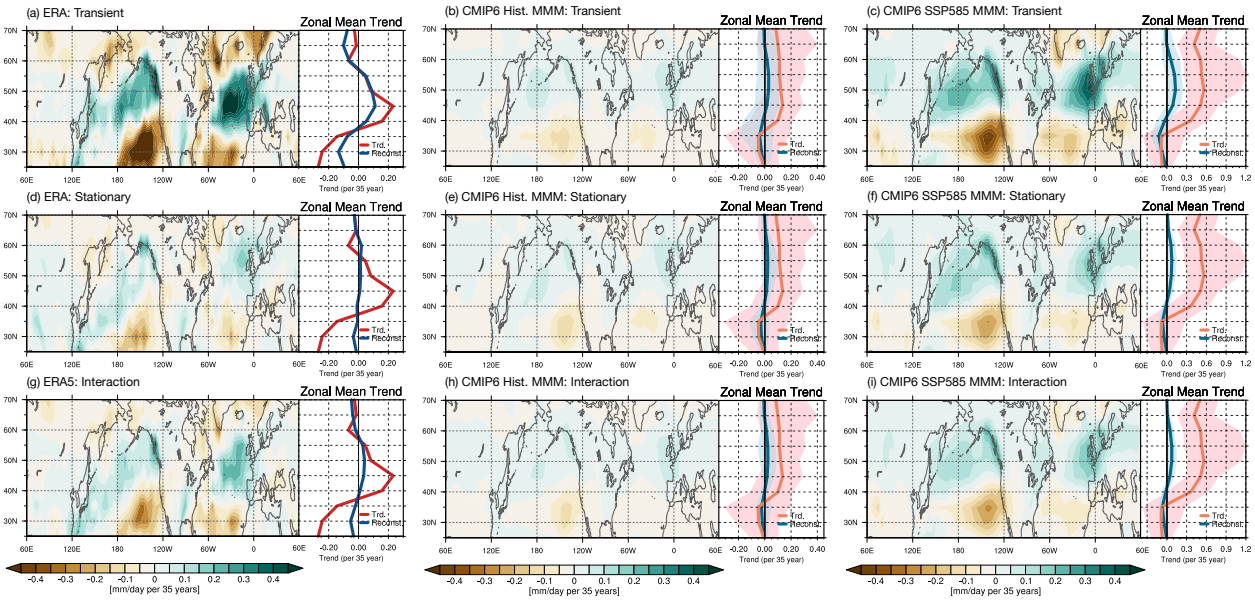

Supplementary Figure 3. Spatial patterns and zonal-mean profiles of decomposed dynamical contributions to total precipitation trends. Each panel shows the total precipitation-trend contribution associated with the (a)–(c) transient, (d)–(f) stationary, and (g)–(i) interaction components. For each component, the left subpanel shows the spatial pattern, and the right subpanel shows the corresponding zonal-mean profile. Columns show (a, d, g) ERA5 (1979–2014), (b, e, h) the CMIP6 historical MMM (21 models, 1979–2014), and (c, f, i) the CMIP6 SSP585 MMM (19 models, 2015–2100). In the zonal-mean subpanels, solid curves denote the component-wise trend ("Trd.") and the corresponding circulation-based reconstruction ("Reconst."). Shading in the CMIP6 zonal-mean subpanels indicates the intermodel range (minimum to maximum). Trend units are mm day^{-1} per 35 years.

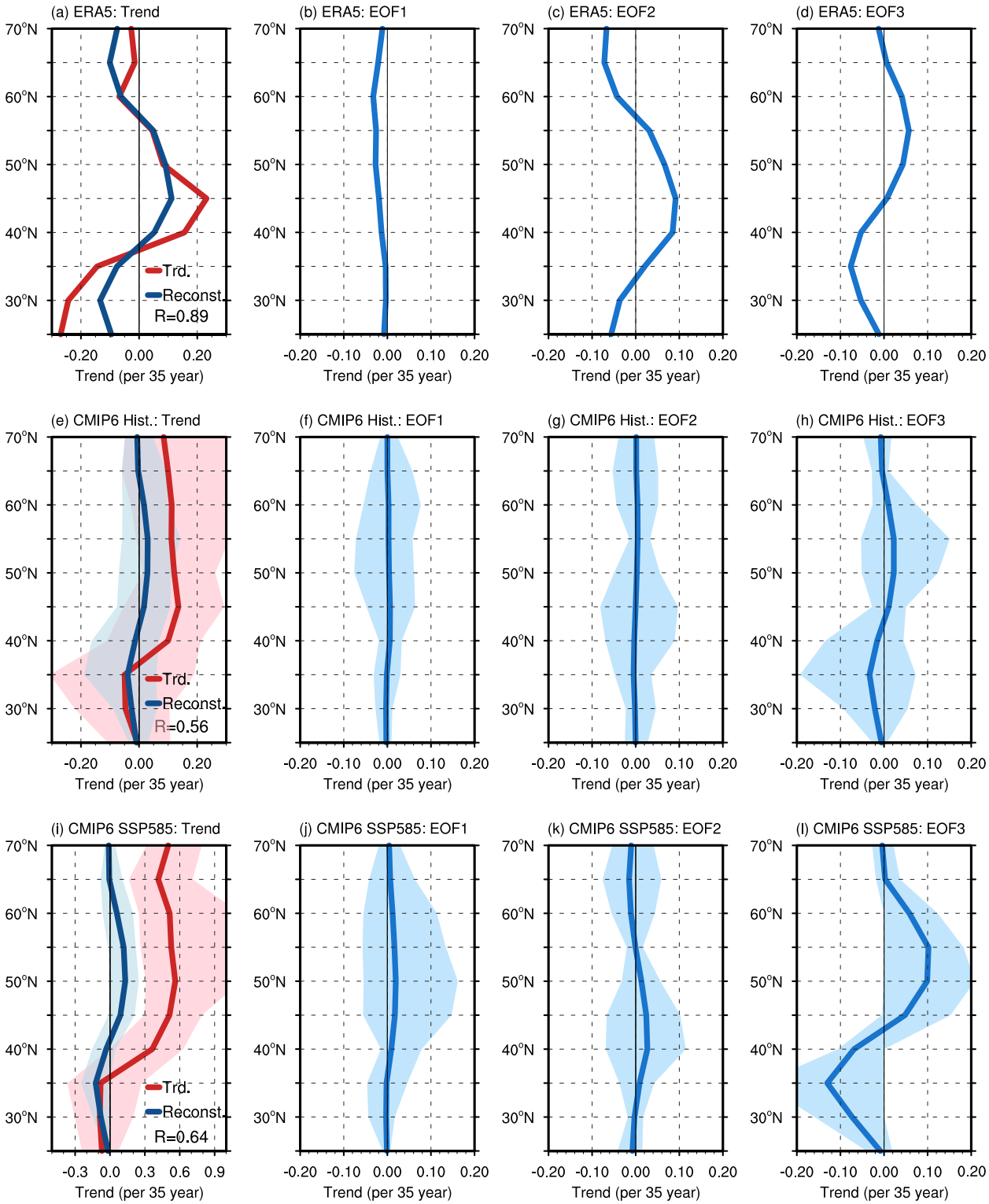

Supplementary Figure 4. Zonal-mean profiles of transient-induced total precipitation trends and EOF-based reconstructions. Zonal-mean profiles are shown for (a)–(d) ERA5 (1979–2014), (e)–(h) the CMIP6 historical MMM (21 models, 1979–2014), and (i)–(l) the CMIP6 SSP585 MMM (19 models, 2015–2100). The first column (a, e, i) compares the transient-induced total precipitation trend ("Trd."; red) with its EOF-based reconstruction ("Reconst."; blue) obtained by summing EOF1–EOF3 contributions; pattern correlation coefficients (R) are shown in each panel. The remaining columns show the zonal-mean

contributions associated with EOF1 (b, f, j), EOF2 (c, g, k), and EOF3 (d, h, l). Shading in the CMIP6 rows indicates the intermodel range (minimum to maximum). Trend units are mm day^{-1} per 35 years.